[Frontiers in Bioscience 18, 970-981, June 1, 2013]

Hematopoietic stem cells improve dopaminergic neuron in the MPTP-mice

Jingwei Lu[1], Suman Kanji[1], Reeva Aggarwal[1], Manjusri Das[1], Matthew Joseph[1], Lai-Chu Wu[2], Hai-Quan Mao[3], Vincent J. Pompili[1], Maria Hadjiconstantinou[4], Hiranmoy Das[1]

[1]Stem Cell Research Laboratory, Cardiovascular Medicine, Davis Heart and Lung Research Institute, Wexner Medical Center at The Ohio State University, Columbus, Ohio 43210, [2]Molecular and Cellular Biochemistry, College of Medicine, Wexner Medical Center at The Ohio State University, Columbus, Ohio, [3]Department of Materials Science and Engineering, John's Hopkins University, Baltimore, MD, [4]Departments of Psychiatry and Pharmacology, Division of Molecular Psychopharmacology, Wexner Medical Center at The Ohio State University, Columbus, Ohio

TABLE OF CONTENT

1. ABSTRACT

Because of their ability for self-renewal and neural differentiation, stem cells are believed to be ideal for cell replacement therapy in Parkinson's disease (PD). Nanofiber-expanded human umbilical cord hematopoietic stem cells (HUHSCs) are advantageous to other stem cells as they provide a source of unlimited stem cell production for clinical application. In this study, we investigated whether 1. nanofiber-expanded HUHSCs are capable of neural differentiation *in vitro*, and 2. they could improve dopaminergic neuron morphology in the caudate/putamen (CPu) and substantia nigra pars compacta (SNc) of the MPTP-mouse model of PD. When cultured under neural differentiation conditions, nanofiber-expanded HUHSCs were able to undergo neural differentiation *in vitro*, as determined by gene and protein expression of neural markers such as MAP2, NeuN, HuC, GFAP and Oligo2. Thirty days after a single intracardioventricular injection of HUHSCs to MPTP-mice there was a significant recovery of tyrosine hydroxylase (TH) immunostaining in CPu. There was an increase in the size and staining density of TH^+ cells in SNc, while their number was unchanged.

2. INTRODUCTION

Despite a half century of intensive basic and clinical research there is no cure for Parkinson's disease (PD). Current pharmacotherapies seek to replace dopamine (DA) deficits primarily with L-DOPA and DA agonists (1, 2). Conventional pharmacological therapies, however, are not curative, have serious side effects and lose efficacy with disease progression (3, 4). Thus, a consensus has emerged for the development of restorative therapies, which could reverse the loss of DA neurons either by preventing the degenerative process and/or by replacing missing or damaged dopaminergic cells (5, 6). Effective restorative therapies are expected not only to reduce damage, but also restore DA transmission and ameliorate abnormal motor function. Cell-based therapies are a promising approach for DA neuron regeneration in PD (7). Over the past two decades animal experiments (8, 9) and human grafting clinical studies (10) have provided the proof-of-principle for the efficacy of primary embryonic dopaminergic neurons and embryonic mesencephalic tissue for cell replacement treatment in PD. However, ethical and medical obstacles with the use of human embryonic tissue

still remain; with limited availability and lack of standardization of the cell material and host rejection being especially critical (11).

Stem cells may provide an alternative source of unlimited production of cells with the potential to acquire DA phenotype *in vitro* or after transplantation *in vivo*. DA cells derived from embryonic or adult stem cells of various sources can survive and reverse behavioral deficits after grafting in animal models of PD (6, 12). Adult stem cells recovered from human umbilical cord, namely hematopoietic stem cells (HUHSCs) and mesenchymal stem cells (HUMSCs), are a valuable source of ethical stem cells with the potential to initiate and maintain tissue repair. Their immaturity and immune naïveté make them unique, safe, less tumorigenic and immunogenic, and suitable for transplantation. Combined with their availability, HUCB cells have been for long viewed as a promising source of autologous/allogenic cell-based therapy for neuroinjury (13). HUMSCs differentiate towards neural lineages and improve neuronal injury in animal models of various neurological disorders (6) including PD (14). In contrast to HUMSCs, little is known about the neural differentiation potential of HUHSCs or their neuroregenerative capacity. Our laboratory has developed a novel *ex vivo* expansion technology by which HUCB-derived hematopoietic ($CD133^+/CD34^+$) stem cells can be expanded more than 225-fold, while preserving stem cell phenotype, characteristics multipotentiallity, and biological functionality (15). This technology allows the generation of millions of hematopoietic stem/progenitor cells for translational application, whereas from a single HUCB less than a million cells can be procured (15, 16). The expanded HUHSCs express high levels of the cell homing receptor CXCR4 as well the adhesion molecule LFA-1 and migrate sufficiently *in vitro* and to the lesion site *in vivo*, and have the ability to bi-potentially differentiate into endothelial and smooth muscle cells (15), and osteoblastic cells (17). In addition, nanofiber-expanded HUHSC therapy enhances angiogenesis in various models of ischemia (15, 18) including stroke (personal observations). In these studies we explored whether nanofiber-expanded HUHCS are able to differentiate into neural lineages *in vitro*, and whether peripheral administration of HUHCS can improve dopaminergic neuron morphology in the caudate/putamen (CPu) and substantia nigra pars compacta (SNc) of the MPTP-mouse model of PD *in vivo*.

3. MATERIALS AND METHODS

3.1. $CD133^+$ cell isolation and *ex-vivo* expansion

Hematopoietic stem cells were isolated and expanded following previously described protocols (15, 16). Specifically, fresh human umbilical cord blood was obtained from The Ohio State University Medical Center after IRB approval and written consent from donors. The heparinized blood was diluted with 1X phosphate buffer (PBS) and layered over 10 ml of Ficoll. After 30 min centrifugation in a swinging bucket rotor at 1400 rpm, the upper layer was aspirated and the mononuclear cell layer collected. Following labeling with magnetic bead conjugated anti-CD133 (CD133) monoclonal antibodies (Miltenyi Biotec Inc, Bergisch Gladbach, Germany) two cell separation cycles were performed using the AutoMACS cell sorter (Miltenyi Biotech Inc) according to the manufacturer's protocol and reagents to isolated $CD133^+$ cells. After separation, purity of the cell product was determined by flow cytometry. For cell expansion, 24-well tissue culture plates with nanofiber meshes securely glued to the bottoms of wells were used (kind gift from Dr. Mao, John's Hopkins University, MD). Eight hundred $CD133^+$ cells were seeded onto each scaffold in 0.6 ml StemSpan™ SFEM serum-free expansion medium (StemCell Technologies, Vancouver, BC, Canada) which consists of 1% BSA, 0.01 mg/ml recombinant human insulin, 0.2 mg/ml human transferrin, 0.1 mM 2-mercaptoethanol and 2 mM l-glutamine in Iscove's modified Dubelco's medium, supplemented with 0.04 mg/ml low-density lipoprotein (Athens Research and Technology Inc., Athens, GA, USA), 100 ng/ml recombinant human stem cell factor (SCF), 100 ng/ml Flt3, 50 ng/ml thombopoietin (TPO) and 20 ng/ml IL-3. SCF, Flt3, TPO and IL-3 were purchased from Peprotech Inc., Rocky Hill, NJ, USA. Cells were cultured at 37 °C in an atmosphere containing 5% CO_2 for 10 days without medium change, and harvested after 10 days of expansion. For the identification of primitive hematopoietic progenitor cell population in the expanded cultures flow cytometry was used. The Milan-Muhlhouse gating method was utilized for cell enumeration and a double gating ($CD133^+$ and $CD34^+$) strategy was employed.

3.2. *In vitro* differentiation of HUHSCs

3.2.1. Cell culture

Nanofiber-expanded HUHSCs (5×10^5/ well) were seeded in a 12-well plate with Hyclone AdvanceSTEM Complete Neural Differentiation Kit (Thermo Fisher Scientific, Inc, Waltham, Massachusetts, USA) containing neural differentiating factors for three weeks. Media were replaced every other day. Phase contrast micrographs were taken to evaluate morphological changes were evaluated at various time point, day 3, day 7, day 15, and day 21. The images were captured under an epifluorescence microscope (Axioplan 2; Carl Zeiss AG, Jena, Germany) using Zeiss Axiovision imaging software.

3.2.2. Scanning electron microscopy

Differentiated cells were also evaluated with scanning electron microscopy (FEI NOVA nanoSEM, FEI Inc., Hillsboro, Oregon, USA) after three weeks *in-vitro* culturing. Briefly, samples were gently rinsed with PBS, fixed with 3% glutaraldehyde for 30 min at 20 °C, and post-fixed with 1% osmium tetraoxide for another 15 min at 20 °C. Samples were then dehydrated using a graded series of ethanol (25%, 50%, 70%, 90%, 95%, 100%, 100%) followed by HMDS drying. The samples were mounted onto aluminum stubs and gold sputter-coated before viewing (19).

3.2.3. RT-PCR

Evaluation of neural specific gene expression was performed at various time points, as indicated in Figures, during the course of differentiation using RT-PCR. Total RNA was isolated using the RNeasy Qiagen Kit (Qiagen,

Venlo, Netherlands). Complementary DNA was synthesized using oligo dT primer (Invitrogen, Carlsbad, CA, USA). The genes for the neural markers MAP2, nestin, GFAP, and Oligo2 were analyzed keeping GAPDH as a control. Primer sequences were as follows: GFAP (F: 5'-GCAGAGATGATGGAGCTCAATGACC-3'; R: 5'-GTTTCATCCTGGAGCTTCTGCCTCA-3'), MAP2 (F: 5'-TCAGAGGCAATGACCTTACC-3'; R: 5'-GTGGTAGGCTCTTGGTCTTT-3'), Olig2 (F: 5'-AAATCGCATCCAGATTTTC-3'; R: 5'-CACTGCCTCCTAGCTTGTC-3'), nestin (F: 5'-AACAGCGACGGAGGTCTCTA-3'; R: 5'-TTCTCTTGTCCCGCAGACTT-3').

3.2.4. Immunofluorescence cytochemistry

Protein expression of neural genes of interest was studied with immunoflorescence cytochemistry at 3 weeks. Cells were fixed with 4% paraformaldehyde at room temperature for 30 min, washed three times with 1XPBS and blocked with 10% goat serum in 1XPBS containing in 0.1% tritonX100 for 30 min. Primary antibodies (GFAP 1:500; Abcam, Cambridge, UK ; MAP2 1:500, Cell Signaling Tech, Danvers, MA, USA; NeuN 1:500; Abcam, Cambridge, UK; HuC, 1:500, Abcam, Cambridge, UK) were added and incubated overnight. Following washings with 1XPBS, cells were incubated with secondary antibody (Alexa Fluor@ 488, 1:250, Invitrogen, Eugene, OR, USA) for 1 h at room temperature in dark and DAPI added. Immunofluorescence was studied under an Axioplan2 epifluorescence microscope, and images captured with a Zeiss Axiovision imaging software (Carl Zeiss AG, Jena, Germany).

3.3. Generation of murine model for Parkinson's disease and HUHSC treatment

Male NOD/SCID mice, 6-8 week old, were used for the studies. They were bred and housed in isolated containment in our laboratory with food and water ad libitum. For the induction of the dopamenergic lesion, mice received four injections of 1 methyl-4-phenyl-1, 2, 3, 6-tetrahyropyrine (MPTP-mice), 20 mg/kg, ip, or saline (intact mice) at 2 h intervals (20). Three days after the lesion, MPTP and intact mice were administered a single intracardioventricular injection of HUHSCs (0.5 x 10^6 cells/mouse in 200 µl serum-free medium) or medium (vehicle) under isofluorane anesthesia. The treatment time was chosen to avoid possible MPTP toxicity on the administered and circulating HUHSCs. The cardioventricular route was used to circumvent cell entrapment in the pulmonary circulation, which is common with tail vein injection (15). Mice were used for immunohistochemical studies 30 days after HUHSC administration. All animal experiments were performed in accordance with guidelines published in the Guide for the Care and Use of laboratory Animals (NRC document), and under the protocol approved by the Institutional Animal Care and Use Committee at the Ohio State University.

3.4. HUHSC homing

Undifferentiated nanofiber-expanded cells were transfected with a luciferase-containing vector using a human CD34 cell Nucleofector kit (Lonza Group AG, Basel, Switzerland) following the manufacturer's protocol. In brief, 1-3 × 10^6 cells were transfected with 2-5 µg of plasmid DNA in 100 µl of CD34 cell Nucleofector solution and using Amaxa electroporator programs: U-008 or U-001 (Lonza Group AG, Basel, Switzerland.). After transfection cells were cultured with serum-free complete DMEM media for 24 h before injection to mice. Based on previous studies (21), MPTP-mice were injected 5 x 10^6 luciferase transfected HUHSCs in medium or medium only intracardioventricularly under isofluorane anesthesia and whole body bioluminescence was assessed 72 h later using a Xenogen *in vivo* imaging system (IVIS, Caliper Life Sciences, Hopkinton, MA, USA). Luciferin, 150 µg/kg, was administered intracardioventricularly immediately prior to imaging under isofluorane anesthesia.

3.5. Immunohistochemistry

Mice were anesthetized with pentobarbital, 50 mg/kg, ip, and perfused transcardially at a flow rate of 10 ml/min^{-1} initially with saline, 3 min, followed by 4% paraformaldehyde solution, 8 min, using a peristaltic pump. Brains were removed and immersed in 4% paraformaldehyde solution overnight. The fixed brains were placed in 30% sucrose in 0.1 M sodium phosphate buffer and cryoprotected by immersion in isopentane (2-methylbutane). Brains were paraffin embedded and sectioned coronally at 10 µm through the midbrain (bregma -2.80 to -3.16 mm according to Paxinos and Franklin, 2001) and striatum (bregma 1.54 to -0.10 mm according to Paxinos and Franklin, 2001) and placed onto Snowcoat X-tra™ glass slides. Prior to staining, slides were incubated in hybridization chambers at 65°C for 1 h, followed by deparaffinization and rehydration. Antigen retrieval was performed using citrate buffer (2.94 g Tri-Sodium citrate, 500 µl Tween-20, pH adjust to 6.0 with 1M HCl) and two cycles of microwave treatment. After peroxidase quenching, sections were blocked for nonspecific staining (5% goat serum, 1% BSA, 0.1% Triton X-100, 0.05% Tween 20 in 1 x PBS) followed by incubation with specific primary and secondary antibodies of interest. Staining was performed by the VECTASTAIN Elite ABC kits (Vector Laboratories Inc, Burlingame, CA) following the manufacturer's protocol. For the immunohistological studies every fourth section was used, and antibodies against the dopamine synthetic enzymes tyrosine hydroxylase (TH; 1:500, Sigma-Aldrich, St. Louis, MO, USA) and aromatic L-amino acid decarboxylase (AAAD; 1:500 PerkinElmer Inc, Waltham, Massachusetts, U.S.) and the astrocytic marker glial fibrillary acid protein (GFAP 1:500; Abcam, Cambridge, UK) were utilized. In some studies the human antibodies (HuNeu 1:500, Millipore, Billerica, MA, USA) were used to detect the presence of HUHSCs in brain. The number of TH^+ positive cells in SNc, the cross-sectional area of their soma, and the density of TH staining per cell were estimated by image analysis (ImageJ, NIH) as we have described (22, 23). TH^+ cells within the boundaries of nucleus A9 were traced manually, and the cross-sectional area of the soma of each cell and the average optical density (OD) of the immunostaining estimated. TH density per cell is expressed as OD/cell soma area for each cell analyzed. The density of TH and AAAD immunostaining in the terminal fields of CPu as well as the

number of TH^+ fibers, expressed as % total area covered, were estimated by image analysis (ImageJ, NIH) after background subtraction and OD calibration (23). The number of $GFAP^+$ cells in CPu was also estimated by image analysis (ImageJ, NIH) following standard methods. Three to 4 sections were used for each antibody, and three sample areas (GFAP: 165 µm X 165 µm, TH 325 µm X 325 µm) examined for each region per section. The number of TH^+ and $GFAP^+$ cells are expressed per mm^2. To avoid intraexperimental variation, brain sections from one set of experimental animals were stained and analyzed together (23). Three animals per treatment group were examined and 3-4 brain sections per animal analyzed.

3.6. Brain microvessel staining

To determine the number of microvessels in brain sections through CPu and midbrain were stained using an alkaline phosphatase kit (Sigma FAST^{TM}BCIP/NTB) following the manufacturer's instructions (15). Image analysis was used to estimate the number of microvessels, estimated in each of 12 randomly chosen high-power fields (HPF) in 3 brain sections for each brain region and animal. Only particles greater than 30 $pixel^2$ were counted to eliminate no specific staining. Results are expressed as the % of the HPF covered by alkaline phosphatase stained microvessels (% of total area covered).

3.7. Statistical analysis

Data were analyzed with one-way ANOVA followed by a Student-Newman-Keuls test for multiple group comparison. For data expressed as percent, the non-parametric Kruskal-Wallis test was used. Analysis was performed with the GraphPad Instat software, and a level of $P<0.05$ was considered as statistically significant.

4. RESULTS

4.1. Nanofiber-expanded HUHSCs differentiate into neural cells

$CD133^+$ cells isolated from freshly collected human umbilical cord blood samples were of greater than 95% purity. They were expanded on nanofiber matrices with a total of 4.5 million cells generated from an initial population of 20,000 cells. During the expansion they maintained the stem cell phenotype and were positive for CD34 and CXCR4 (15). When cultured in neural differentiation media for three weeks, nanofiber-expanded HUHSCs underwent morphological changes suggestive of neural differentiation. Morphological changes were present in day 3 and by day 21 the majority of the cells displayed neuronal or glial appearance, which was also confirmed with scanning electron microscopy (Figure 1a, b, and c). RT-PCR analysis demonstrated the expression of neural lineage specific genes, such as GFAP for astrocytes, MAP2 for neurons, oligo2 for oligodendrocyes, and nestin, for neuronal and endothelial cells, during the differentiation period (Figure 1d). No appreciable mRNA for GFAP, MAP2 and Oligo2 was observed in control undifferentiated HUHSCs. Detectable GFAP mRNA expression was seen at day 7-10 and then declined. In contrast, oligo2 mRNA increased with time in culture. MAP2 mRNA expression was evident by day 3 and remained stable for the duration of the studies. Control HUHSCs expressed nestin mRNA and its levels were not substantially altered in HUHSCs undergoing differentiation. Immunofluorescence microscopy showed that GFAP and MAP2 proteins were expressed in differentiated HUHSCs three weeks in culture (Figure 2), indicating that neural-specific gene expression is accompanied by translation. Two other neuronal specific proteins, the neuronal nuclear antigen NeuN and the neuron specific member of the Hu family, HuC were also detected in differentiated HUHSCs after 3 weeks of culturing (Figure 2). Taken together, the data provide evidence for neural differentiation of nanofiber-expanded HUHSCs *in vitro*.

4.2. HUHSCs' homing after intracardioventricular administration to mice

Previous studies showing that following peripheral administration nanofiber-expanded HUHSCs preferentially home in the site of a lesion *in vivo*, for example in the brain after stroke or in the hind limb after ischemia [personal observations; (15), provided the rational for the question whether HUHSCs could home in the brain after an MPTP injury to dopaminergic neurons. MPTP-mice were administered 5×10^6 luciferase transfected HUHSCs in medium or vehicle and whole body bioluminescence was evaluated by IVIS imaging 72 h later. Bioluminescence of various intensities was detected in distinct regions of the MPTP-mouse body, prominently in the head (Figure 3). Luciferase activity was consistently observed in the head area of the HUHSC-injected mice, and the estimated signal was brighter than that detected in other body areas. In several studies, we have observed no bioluminescence in the head or body of intact control mice treated with luciferase transfected HUHSCs with low levels of activity detected in the tail and paws apparently reflecting circulating HUHSCs (personal observations). We interpreted our imaging findings to indicate that a significant number of HUHSCs home to head tissues, such as vasculature and brain, and that factors associated with the MPTP-induced lesion act as stem cell attractants. Peripheral MPTP toxicity might be accounted for the moderate accumulation of luciferase transfected HUHSCs in the upper and lower body of the MPTP-mice. No bioluminescence signal was detected following luciferin injection to mice not treated with luciferase transfected HUHSCs.

4.3. HUHSC improves the size of nigral dopaminergic neurons and recovers TH immunostaining density in the SNc and CPu of the MPTP-mice

Based on the imaging results of significant HUHSCs homing in the mouse head after a single intracardioventricular injection and reports that HUHSCs are capable of crossing the blood brain barrier (BBB) (24), we hypothesized that circulating HUHSCs may home in brain parenchyma of the MPTP-mice, particularly when BBB is disrupted in these animals (25, 26). A reasonable inference of HUHSCs' homing in the brain of the MPTP-mice is that they may migrate to the lesioned striatum and/or midbrain where, they could either differentiate into neurons or influence residual dopaminergic neuron number and morphology by eliciting neurotrophic signaling. To

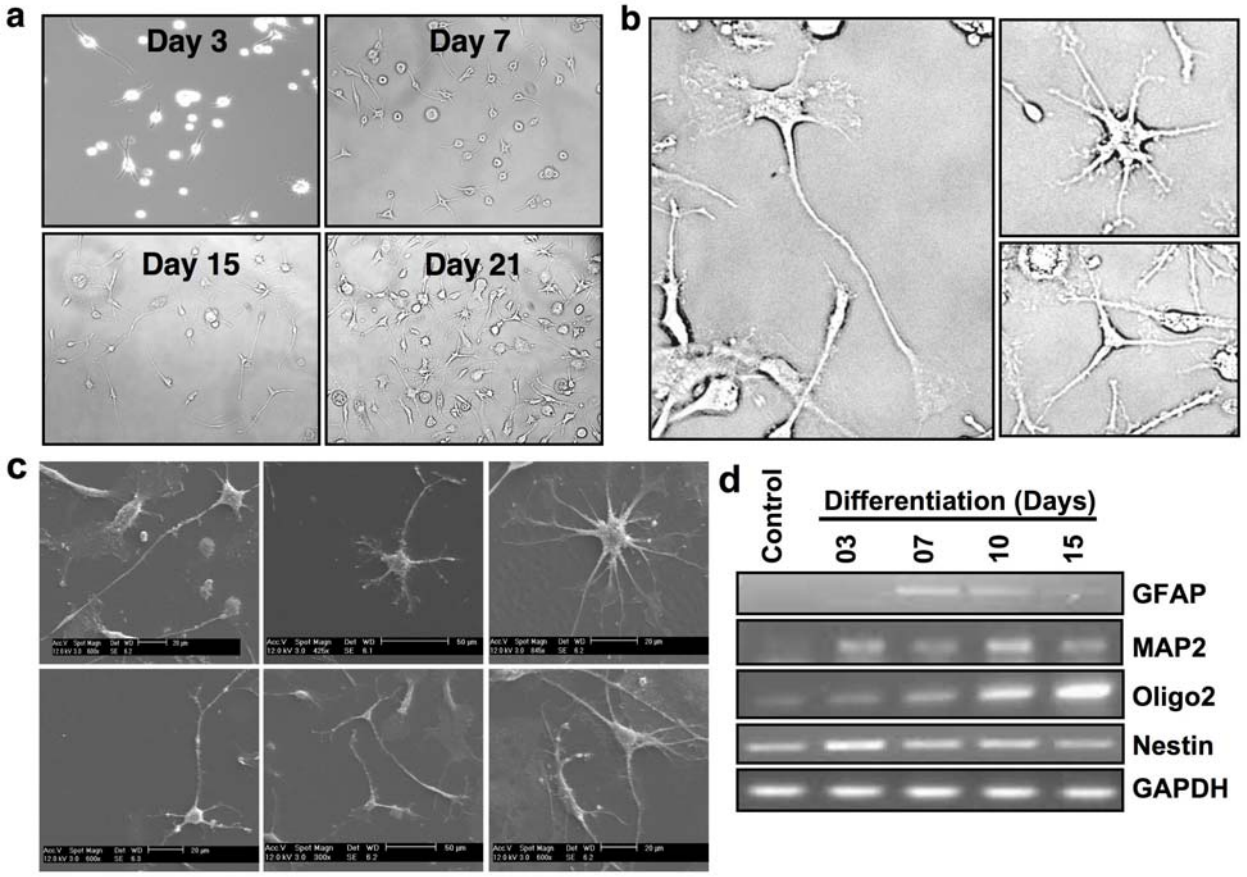

Figure 1. Neural differentiation of nanofiber-expanded hematopoietic stem cells. Nanofiber-expanded HUHSCs were cultured in neural differentiation media for 21 days, as described in methods. a. Light microscope images depicting morphological changes at various time points during differentiation (3, 7, 15 and 21 days). b. Light microscope images depicting cells with neuronal (left panel) and glial (right panels) features on day 21 in culture. c. Scanning electron microscope images depicting cells with neuronal (left 4 panels) and glial (right 2 panels) features after 3 weeks in culture. d. Neuroglial characterization of HUHSC *in vitro*. RT-PCR expression of differentiated (MAP2, GFAP, Oligo2) and undifferentiated (nestin) neural genes at various time points during differentiation (3, 7, 10 and 15 days). GAPDH serves as an internal control.

explore these possibilities, undifferentiated nanofiber-expanded HUHSCs were administered intracardioventricularly once to MPTP-mice 3 days after the MPTP treatment, and TH immunohistochemistry performed 30 days later. Following MPTP there was a significant loss of TH^+ cells in SNc (Figure 4a and b), as expected (20, 22). Morphometric studies demonstrated a significant reduction in the calculated cross-sectional area of the soma of TH^+ neurons in the lesioned SNc (Figure 4c), which under the microscope appeared shrunk with irregular shape. HUHSC treatment had no effect on cell number (Figure 4a and b), but it partially reversed the shrinkage of the residual dopaminergic cells in SNc (Figure 4c). Furthermore, following the stem cell treatment, there was an almost complete recovery of the decreased TH protein expression in the nigral neurons, as indicated by the OD measurements of TH immunostaining in individual cells (Figure 4d).

The MPTP treatment caused a significant decrease in TH immunoreactivity in CPu (Figure 5a) that was due to a reduction of dopaminergic terminals and TH expression (Figure 5b and c). Treatment with HUHSCs partially attenuated the loss of TH immunoreactivity (Figure 5a, b and c). This was apparently due to up-regulated TH expression in the residual dopaminergic neurons, as the number of TH^+ fibers, expressed as % of area covered, was not altered by the stem cell treatment. The immunostaining of L-DOPA decarboxylase, the second enzyme in the biosynthetic pathway of dopamine, was within control values 30 days after MPTP reflecting differential up-regulation of the dopamine synthetic enzymes following MPTP (27, 28), and HUHSC treatment had no effect (data not shown). Using human HuNu, we were not able to identify HUHSCs in midbrain, striatum or other brain regions (data not shown).

4.4. HUHSC treatment has no effect on the MPTP-induced increase of $GFAP^+$ cells in CPu

Thirty days after MPTP, there was a moderate increase in the $GFAP^+$ cells in CPu (Figure 6a and b), as it has been reported (29), and treatment with HUHSCs had no effect (Figure 6a and b).

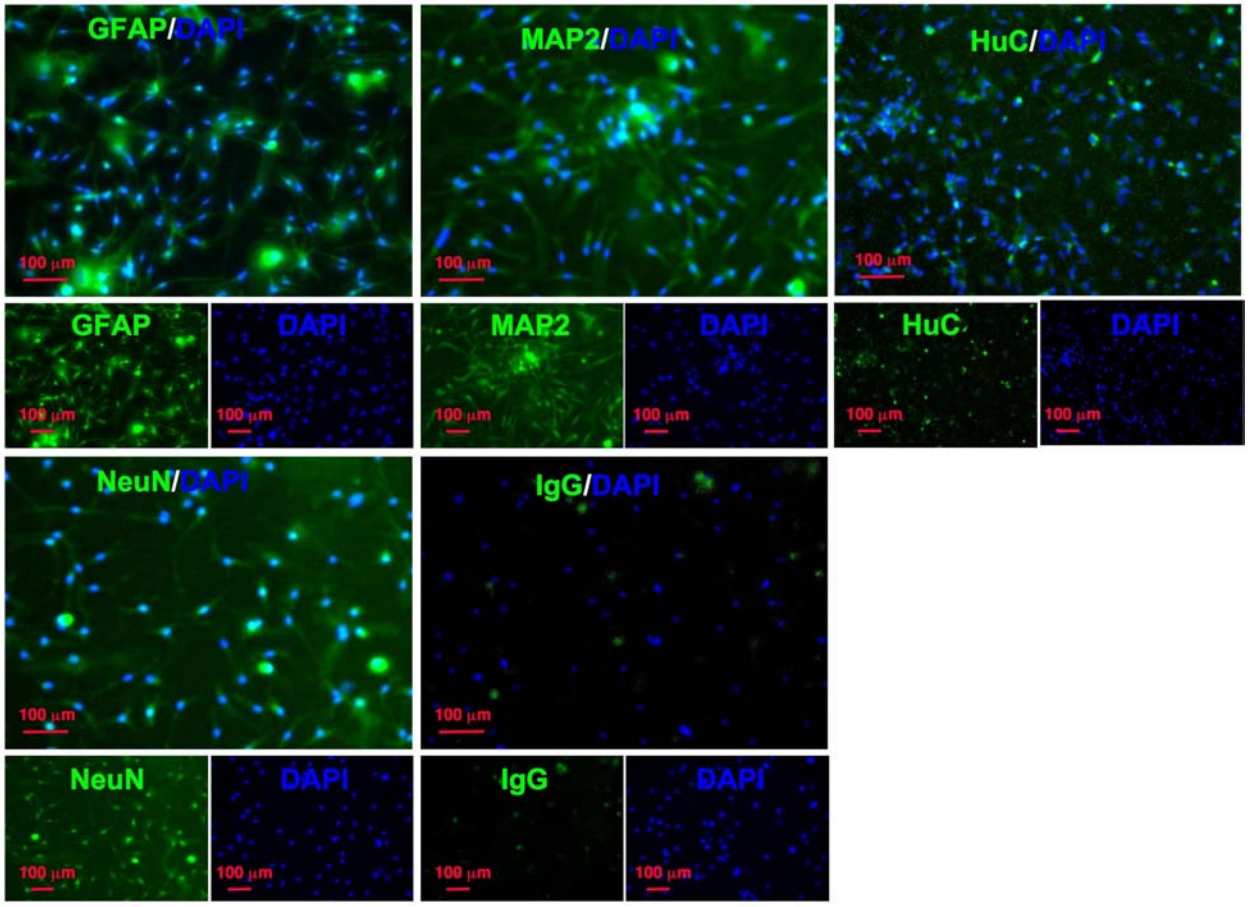

Figure 2. Immunocytochemical evidence of HUHSC neuronal and glial differentiation. Nanofiber- expanded HUHSCs were cultured in neural differentiation media for 21 days and subjected to immunofluorescent staining for neuronal, MAP2, NeuN and HuC, and glial, GFAP markers, as described in methods. Alexa fluor 488 was used as a conjugated fluorescent molecule in secondary antibody. Nuclear staining was performed with DAPI.

4.5. HUHSCs cause angiogenesis in CPU and midbrain

Because our previous studies with ischemic models have shown that HUHSCs are capable of inducing angiogenesis (15), we asked whether this might be also true in the brain of the MPTP-mouse. Toward this goal, brain sections were stained with alkaline phosphatase and the density of brain microvessels was estimated in SNc and CPu. When expressed as % total area covered, there was a significant reduction in the density of microvessels in SNc (Figure 7a) and CPu (Figure 7b) of the MPTP-mice. Microvessel density increased 30 days after HUHSC treatment and approached control values in both SNc and CPu (Figure 7a and b) suggesting angiogenesis. It appears that the HUHSC-induced neovascularization was associated with the MPTP-lesion, as no changes were observed in areas of cortex not affected by the toxin (data not shown).

5. DISCUSSION

These studies provide evidence supporting the notion that HUHSCs are differentiated to neural lineages *in vitro*, and enhance dopaminergic neuron morphology after an MPTP lesion *in vivo*. Indeed, under the neural differentiation conditions used, HUHSCs underwent dramatic morphological changes with a sizeable cell population resembling neurons, while oligodendrocyte- and astrocyte-like cells were also observed. Differentiation was evident by day 3 in culture with the majority of stem cells having acquired neural morphology and characteristics 3 weeks later, the longest time studied. In agreement with the phenotypic morphological changes, during the differentiation there was a parallel expression of three neural specific genes, MAP2, GFAP and Oligo2 detected at the mRNA and protein levels. Our observation that the early neuronal marker HuC and the mature neuronal marker NeuN were also expressed in the differentiated HUHSCs provides further support for the potentiality of the cells to differentiate toward neuronal lineage. Reportedly, $CD133^{+}$ HSCs could be induced to express neuronal, astrocytic and oligodendroglial markers by treatment with retinoic acid and adult hematopoietic cells migrated into the brain after transplantation were found positive for microglial and astroglial markers (30).

The HUHSCs' capacity for neuronal differentiation along with their homing ability in the lesion

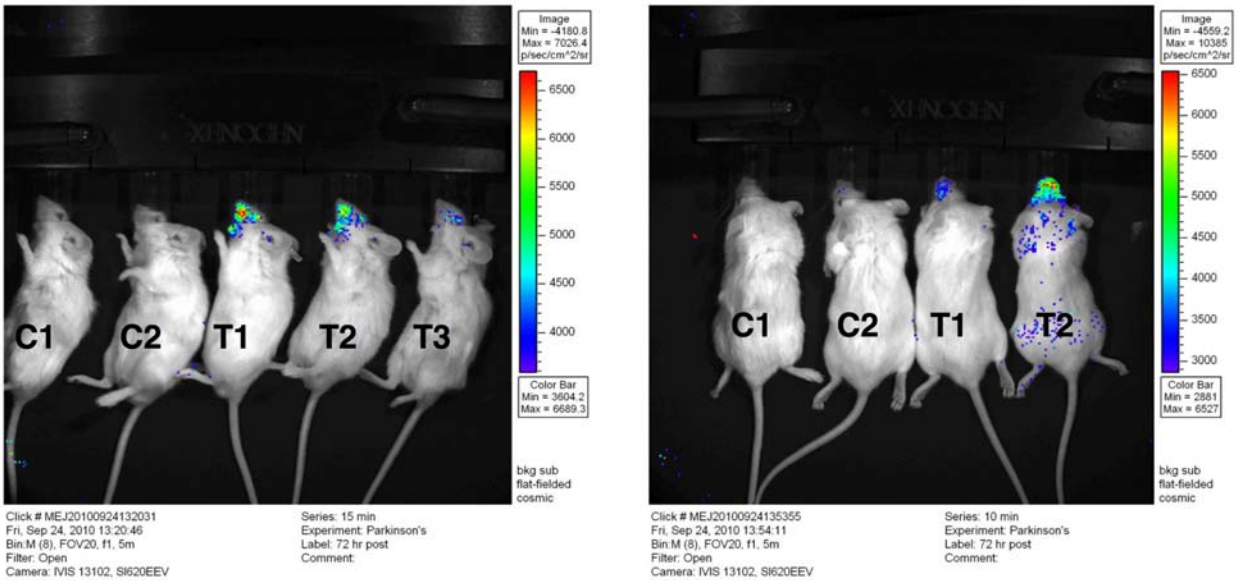

Figure 3. HUHSC homing in MPTP-mice. Mice were treated with MPTP and 3 days later injected once with lucifereace-transfected undifferentiated HUHSCs (T) or medium (C) intracardioventricularly, as described in methods. Whole body bioluminescence was detected with an IVIS imaging system 3 days later, as described in methods. Left panel is the side view of the animals. Right panel is the dorsal view of the animals.

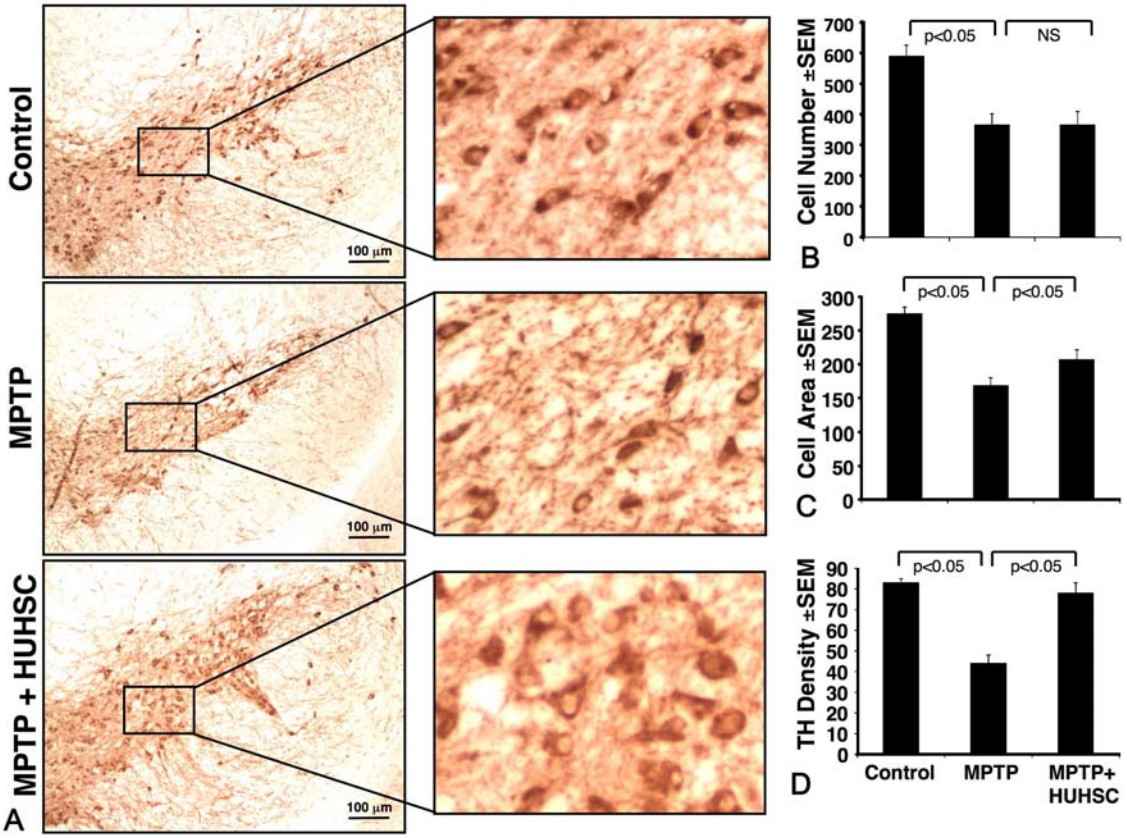

Figure 4. HUHSC treatment enhances cell size and TH density of dopaminergic neurons in the SNc of MPTP-mice. MPTP-mice were treated with HUHSCs or medium once intracardioventricularly 3 days after MPTP administration, as described in methods. The number and size of TH^+ cells in SNc as well as the optical desnity (OD) of TH immunostaining were estimated by image analysis 30 days after the treatment, as described in methods. a. TH^+ cells in the SNc of control, MPTP and MPTP+ HUHSC mice. Right panels are the blown-up images. b. Number of TH^+ cells/mm^2. c. Size of TH^+ cells expressed as the cross sectional soma area in $pixel^2$. d. Cell TH immunostaining density, expressed as OD/cell area. N= 3 animals/group.

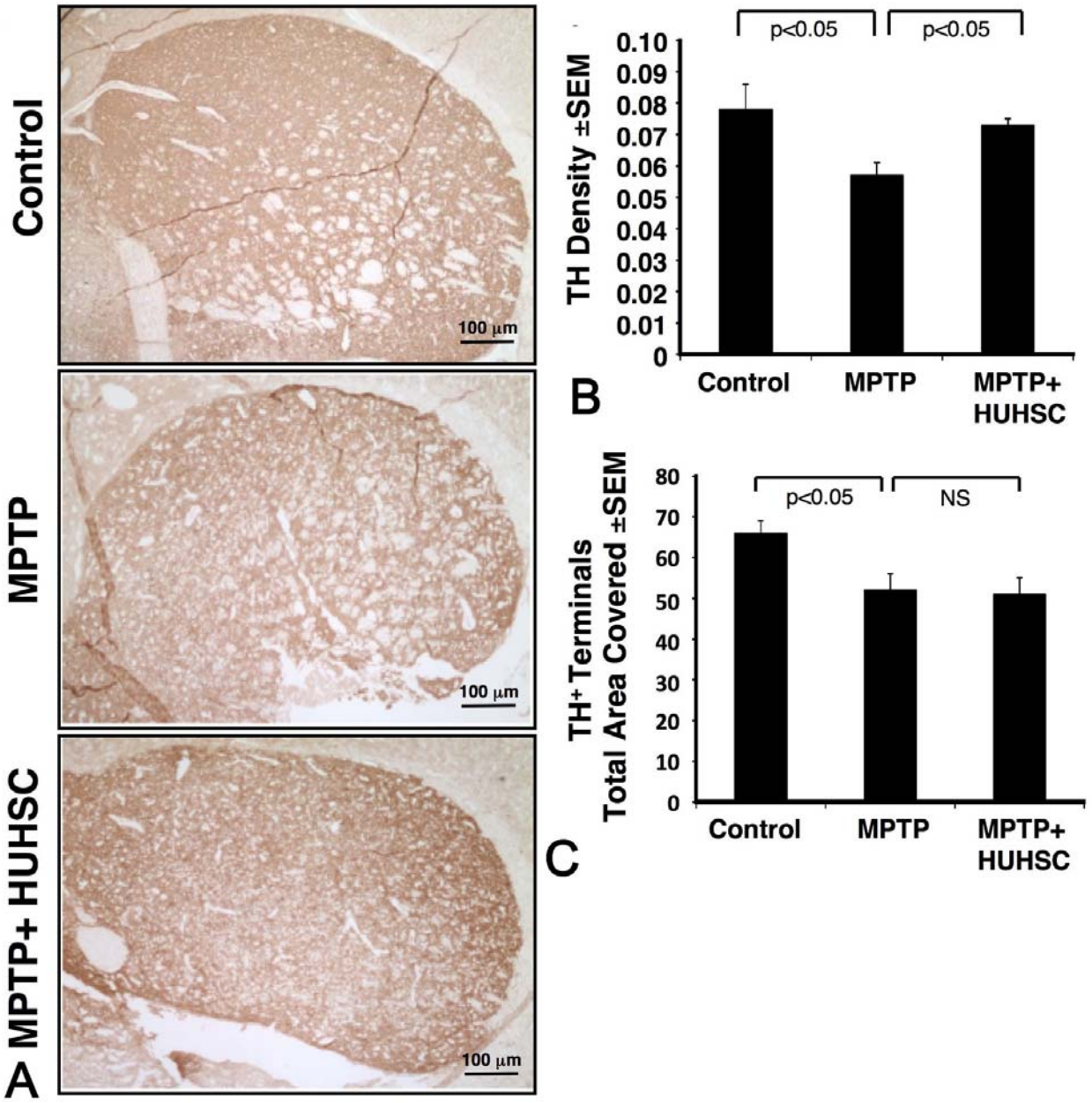

Figure 5. HUHSC treatment recovers TH immunostaining loss in the CPu of MPTP-mice. MPTP-mice were treated with HUHSCs or medium once intracardioventricularly 3 days after MPTP administration, as described in methods. The number of TH^+ fibers and the optical desnity (OD) of TH immunostaining in CPu were estimated by image analysis 30 days after the treatment, as described in methods. a. TH immunostaining in the CPu of control, MPTP and MPTP+HUHSC mice. b. Optical density (OD) of TH^+ fibers in CPu expressed as $OD/pixel^2$. C. Number of TH^+ Fibers expressed as % of CPu area covered. N=3 animals/group.

site *in vivo* (15) provided the basis for their consideration as a putative restorative therapy for neurodegenerative diseases, including PD, which we are currently exploring in various injury animal models. The presented *in vivo* studies with the MPTP-mouse are the first evidence demonstrating the neurorestorative potential of HUHSCs. Peripheral administration of HUHSCs improved the size and altered morphology of the lesioned dopaminergic neurons in the SNc and enhanced TH expression without affecting cell number suggesting metabolic and phenotypic up-regulation (31). Similarly, there was an increased in TH immunoreactivity in CPu that is suggestive of increased TH protein levels in the residual dopaminergic terminals, as the number of dopaminergic terminals did not change after the stem cell treatment. Together the morphological findings strongly support the idea that that HUHSC treatment

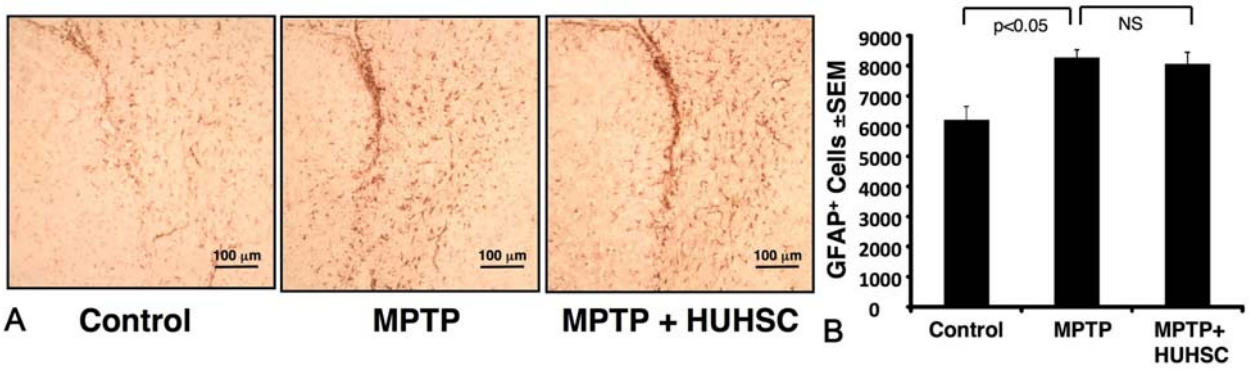

Figure 6. GFAP$^+$ cells in the CPu of MPTP-mice. MPTP-mice were treated with HUHSCs or medium once intracardioventricularly 3 days after MPTP administration, as described in methods. The number of GFAP$^+$ cells in CPu was estimated by image analysis 30 days after the treatment, as described in methods. a. GFAP immunostaining in control, MPTP and MPTP+HUHSC mice. b. Number of GFAP$^+$ cells/mm^2. N=3 animals/group.

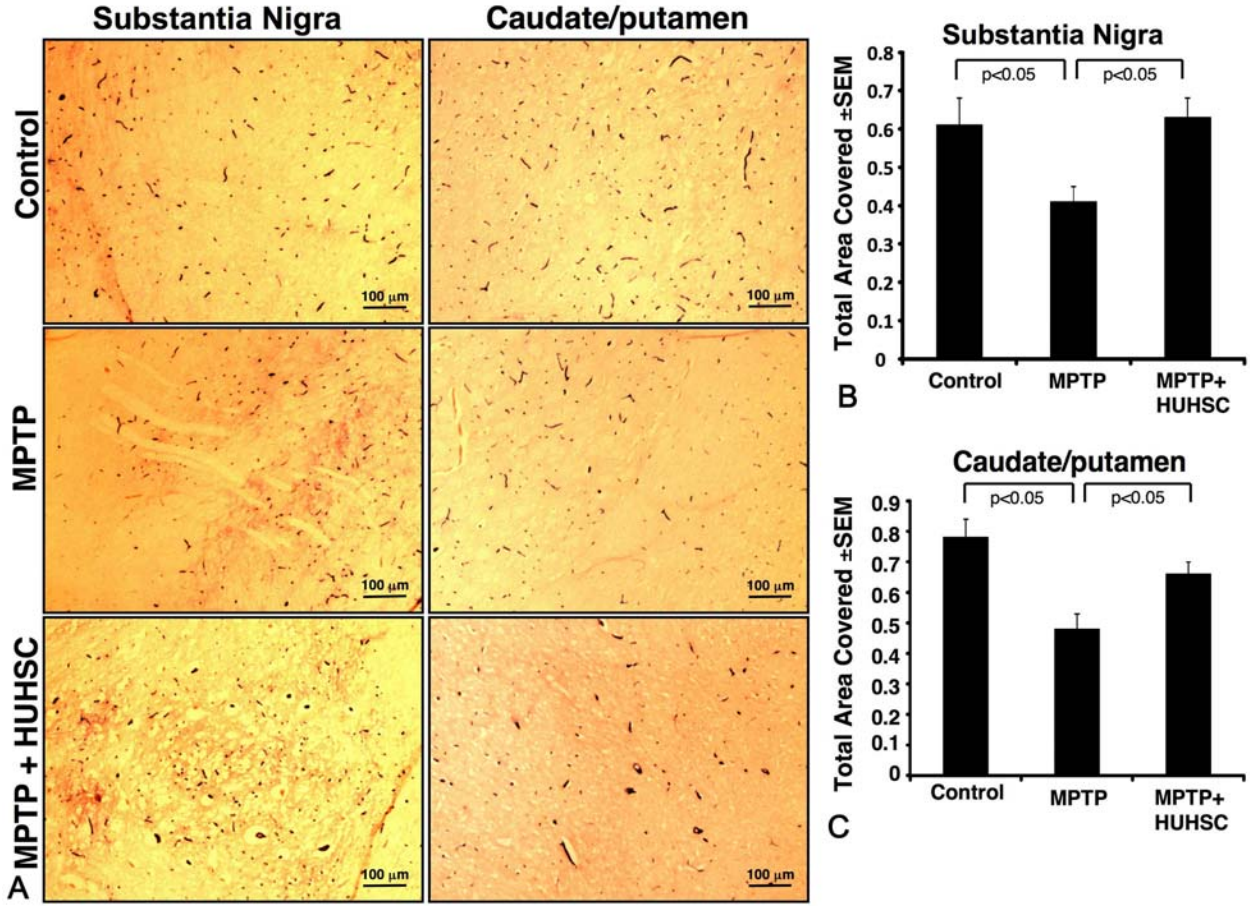

Figure 7. HUHSC-induced angiogenesis in the SNc and CPu of MPTP-mice. MPTP-mice were treated with HUHSCs or medium once intracardioventricularly 3 days after MPTP administration, as described in methods. Brain microvessels were stained with alkaline phosphatase and their number in midbrain and CPu estimated by image analysis, as described in methods. a. Alkaline phosphatase stained microvessels in SNc of control, MPTP and MPTP+HUHSC mice (left panel). Number of microvessels, expressed as % of total area of SNc covered, in SNc (right panel). b. Alkaline phosphatase stained microvessels in CPu of control, MPTP and MPTP+HUHSC mice (left panel). Number of microvessels, expressed as % of total area of CPu covered, in CPu (right panel). N=3 animals/group.

enhances the recovery of lesioned DA neurons in the MPTP-mouse model of PD.

Although the imaging studies pointed to possible stem cell homing in brain tissues 3 days after their administration to MPTP-mice, we were not able to detect HUHSCs in the brain parenchyma 30 days later using human NeuN (personal observations). The absence of HUHSCs in the brain parenchyma could be interpreted as 1) lack of migration, or 2) short life span of migrated cells. The fate of HUHSCs in the MPTP-mouse brain over the time is under investigation. Peripherally administered HUHSCs could adhere to brain microvessels via endothelial adhesion molecules, such as ICAM-1 (15, 32) and subsequently transmigrate to brain parenchyma where they could be attracted to SDF-1 producing cells, such as DA neurons and glia (33, 34) via chemotaxis (35) and alter their trophic milieu and responses. Alternatively, it is possible that factors released by circulating HUHSCs contribute to the observed effect on lesioned dopaminergic neurons. Neuroprotection and neurorestoration by HUCB-based cell treatment does not require cell homing in the lesioned brain in stroke models (36), and this may be true in the MPTP-mouse. The HUHSC effect might be direct by releasing trophic factors for DA neurons (37), and/or indirect by inducing and/or upregulating intrinsic dopaminergic trophic activity in the brain. Neuroinflammation is central to MPTP-neurotoxicity and antiinflammatory drugs reportedly prevent dopaminergic neuron degeneration (38, 39). Our observation of gliosis in the striatum of both HUHSC treated and untreated MPTP-mice suggest that the stem cell effect is independent of the inflammatory process.

MPTP causes capillary and arterioral endothelial damage (40) that affects BBB function (41) and decreases the density of brain microvessels (42). Reduced nutrient uptake, hypoxia and free radicals have been proposed to be involved in the MPTP neurotoxicity and DA neurons are sensitive to hypoxia/ischemia (43, 44). The observed HUSHC-induced angiogenesis in SNc and CPu may contribute to dopaminergic neuron recovery. Remodeling of the neurovasculature could contribute to the dopaminergic restorative/regenerative process by enhancing cerebral blood flow, providing needed nutrients, and clearing toxic cell by products (45). Notably, angiogenesis has been associated with improved motor function after exercise in MPTP-mice (42). Human umbilical blood cord cells secreted angiogenic factors (37) are likely responsible for the observed neovascularization in the SNc and CPu of the MPTP-mice (46).

In summary, our studies provide experimental evidence that peripheral administration of HUHSCs promotes the morphological recovery of lesion dopaminergic neurons and induce angiogenesis in the SNc and CPu of the MPTP-mouse model of PD. Our findings are significant as they are the first preclinical demonstration of the utility of nanofiber-expanded HUHSCs as cell-based restorative therapy for PD, and can be viewed as a step forward in the effort to discover suitable stem cell populations for transplantation. The nanofiber-expanded HUHSCs used are ethical and meet the requirements set for optimal cell-base treatment therapeutic outcome. The observation, that DA neuron injury by MPTP coincided with decreased vascularization SNc and CPu while recovery by HUHSCs with revascularization supports a role of the vasculature in the degenerative/regenerative process. The present studies focused on establishing the morphological recovery of dopaminergic neurons and we can only conjure on the underlying mechanisms. The data support phenotypic upregulation of the residual dopaminergic neurons 30 days after the lesion. Whether the neurotrophic signaling was triggered by short-lived HUHSCs migrated into the lesion site or by HUHSCs homed in brain microvessels is under investigation.

6. ACKNOWLEDGEMENTS

This work was supported in part by National Institutes of Health grants, K01 AR054114 (NIAMS), SBIR R44 HL092706-01 (NHLBI), R21 CA143787 (NCI) and The Ohio State University start-up fund. The funders had no role in study design, data collection and analysis, decision to publish or preparation of the manuscript.Authors have no competing financial interests except Dr. Vincent Pompili, who has equity interest of Arteriocyte Inc. Cleveland, OH.

7. REFERENCES

1. M. Hadjiconstantinou and N. H. Neff: Enhancing aromatic L-amino acid decarboxylase activity: implications for L-DOPA treatment in Parkinson's disease. *CNS Neurosci Ther*, 14(4), 340-51 (2008)

2. S. Perez-Lloret and O. Rascol: Dopamine receptor agonists for the treatment of early or advanced Parkinson's disease. *CNS Drugs*, 24(11), 941-68 (2010)

3. G. Fabbrini, J. M. Brotchie, F. Grandas, M. Nomoto and C. G. Goetz: Levodopa-induced dyskinesias. *Mov Disord*, 22(10), 1379-89; quiz 1523 (2007)

4. G. Pezzoli and M. Zini: Levodopa in Parkinson's disease: from the past to the future. *Expert Opin Pharmacother*, 11(4), 627-35 (2010)

5. L. Aron and R. Klein: Repairing the parkinsonian brain with neurotrophic factors. *Trends Neurosci*, 34(2), 88-100 (2011)

6. A. K. Meyer, M. Maisel, A. Hermann, K. Stirl and A. Storch: Restorative approaches in Parkinson's Disease: Which cell type wins the race? *Journal of the Neurological Sciences*, 289(1-2), 93-103 (2010)

7. A. Bjorklund, S. B. Dunnett, P. Brundin, A. J. Stoessl, C. R. Freed, R. E. Breeze, M. Levivier, M. Peschanski, L. Studer and R. Barker: Neural transplantation for the treatment of Parkinson's disease. *Lancet Neurol*, 2(7), 437-45 (2003)

8. O. Lindvall: Clinical application of neuronal grafts in Parkinson's disease. *J Neurol*, 242(1 Suppl 1), S54-6 (1994)

9. C. Winkler, D. Kirik, A. Bjorklund and S. B. Dunnett: Transplantation in the rat model of Parkinson's disease: ectopic versus homotopic graft placement. *Prog Brain Res*, 127, 233-65 (2000)

10. P. Brundin, R. A. Barker and M. Parmar: Neural grafting in Parkinson's disease Problems and possibilities. *Prog Brain Res*, 184, 265-94 (2010)

11. O. Lindvall and Z. Kokaia: Prospects of stem cell therapy for replacing dopamine neurons in Parkinson's disease. *Trends in Pharmacological Sciences*, 30(5), 260-7 (2009)

12. Y. S. Levy, M. Stroomza, E. Melamed and D. Offen: Embryonic and adult stem cells as a source for cell therapy in Parkinson's disease. *Journal of Molecular Neuroscience*, 24(3), 353-385 (2004)

13. D. T. Harris: Cord blood stem cells: a review of potential neurological applications. *Stem Cell Rev*, 4(4), 269-74 (2008)

14. Y. S. Fu, Y. C. Cheng, M. Y. Lin, H. Cheng, P. M. Chu, S. C. Chou, Y. H. Shih, M. H. Ko and M. S. Sung: Conversion of human umbilicacord mesenchymal stem cells in Wharton's jelly to dopaminergic neurons *in vitro*: potential therapeutic application for Parkinsonism. *Stem Cells*, 24(1), 115-24 (2006)

15. H. Das, N. Abdulhameed, M. Joseph, R. Sakthivel, H. Q. Mao and V. J. Pompili: *Ex vivo* nanofiber expansion and genetic modification of human cord blood-derived progenitor/stem cells enhances vasculogenesis. *Cell Transplant*, 18(3), 305-18 (2009)

16. J. Lu, R. Aggarwal, V. J. Pompili and H. Das: A novel technology for hematopoietic stem cell expansion using combination of nanofiber and growth factors. *Recent Pat Nanotechnol*, 4(2), 125-35 (2010)

17. R. Aggarwal, J. Lu, S. Kanji, M. Joseph, M. Das, G. J. Noble, B. K. McMichael, S. Agarwal, R. T. Hart, Z. Sun, B. S. Lee, T. J. Rosol, R. Jackson, H.-Q. Mao, V. J. Pompili and H. Das: Human Umbilical Cord Blood-Derived CD34+ Cells Reverse Osteoporosis in NOD/SCID Mice by Altering Osteoblastic and Osteoclastic Activities. *PLoS One*, 7(6), e39365 (2012)

18. H. Das, J. C. George, M. Joseph, M. Das, N. Abdulhameed, A. Blitz, M. Khan, R. Sakthivel, H. Q. Mao, B. D. Hoit, P. Kuppusamy and V. J. Pompili: Stem cell therapy with overexpressed VEGF and PDGF genes improves cardiac function in a rat infarct model. *PLoS One*, 4(10), e7325 (2009)

19. K. N. Chua, C. Chai, P. C. Lee, Y. N. Tang, S. Ramakrishna, K. W. Leong and H. Q. Mao: Surface-aminated electrospun nanofibers enhance adhesion and expansion of human umbilical cord blood hematopoietic stem/progenitor cells. *Biomaterials*, 27(36), 6043-51 (2006)

20. V. Jackson-Lewis and S. Przedborski: Protocol for the MPTP mouse model of Parkinson's disease. *Nat Protoc*, 2(1), 141-51 (2007)

21. X. L. Wang, M. Rosol, S. D. Ge, D. Peterson, G. McNamara, H. Pollack, D. B. Kohn, M. D. Nelson and G. M. Crooks: Dynamic tracking of human hematopoietic stem cell engraftment using *in vivo* bioluminescence imaging. *Blood*, 102(10), 3478-3482 (2003)

22. M. Hadjiconstantinou, A. P. Mariani and N. H. Neff: GM1 ganglioside-induced recovery of nigrostriatal dopaminergic neurons after MPTP: an immunohistochemical study. *Brain Res*, 484(1-2), 297-303 (1989)

23. V. M. Goettl, T. A. Wemlinger, A. M. Duchemin, N. H. Neff and M. Hadjiconstantinou: GM1 ganglioside restores dopaminergic neurochemical and morphological markers in aged rats. *Neuroscience*, 92(3), 991-1000 (1999)

24. M. A. Eglitis and E. Mezey: Hematopoietic cells differentiate into both microglia and macroglia in the brains of adult mice. *Proceedings of the National Academy of Sciences of the United States of America*, 94(8), 4080-4085 (1997)

25. C. H. Zhao, Z. D. Ling, M. B. Newman, A. Bhatia and P. M. Carvey: TNF-alpha knockout and minocycline treatment attenuates blood-brain barrier leakage in MPTP-treated mice. *Neurobiology of Disease*, 26(1), 36-46 (2007)

26. X. Chen, X. Lan, I. Roche, R. Liu and J. D. Geiger: Caffeine protects against MPTP-induced blood-brain barrier dysfunction in mouse striatum. *J Neurochem*, 107(4), 1147-57 (2008)

27. M. Hadjiconstantinou and N. H. Neff: Differential recovery of dopamine synthetic enzymes following MPTP and the consequences of GM1 ganglioside treatment. *Eur J Pharmacol*, 181(1-2), 137-9 (1990)

28. D. T. Stephenson, M. A. Childs, Q. Li, S. Carvajal-Gonzalez, A. Opsahl, M. Tengowski, M. D. Meglasson, K. Merchant and M. E. Emborg: Differential loss of presynaptic dopaminergic markers in Parkinsonian monkeys. *Cell Transplant*, 16(3), 229-44 (2007)

29. J. F. Reinhard, Jr., D. B. Miller and J. P. O'Callaghan: The neurotoxicant MPTP (1-methyl-4-phenyl-1,2,3,6-tetrahydropyridine) increases glial fibrillary acidic protein and decreases dopamine levels of the mouse striatum: evidence for glial response to injury. *Neurosci Lett*, 95(1-3), 246-51 (1988)

30. Y. K. Jang, J. J. Park, M. C. Lee, B. H. Yoon, Y. S. Yang, S. E. Yang and S. U. Kim: Retinoic acid-mediated induction of neurons and glial cells from human umbilical cord-derived hematopoietic stem cells. *J Neurosci Res*, 75(4), 573-84 (2004)

31. M. Hadjiconstantinou, P. Panula, Z. Lackovic and N. H. Neff: Spinal cord serotonin: a biochemical and immunohistochemical study following transection. *Brain Res*, 322(2), 245-54 (1984)

32. P. Turowski, P. Adamson and J. Greenwood: Pharmacological targeting of ICAM-1 signaling in brain endothelial cells: potential for treating neuroinflammation. *Cell Mol Neurobiol*, 25(1), 153-70 (2005)

33. G. Banisadr, D. Skrzydelski, P. Kitabgi, W. Rostene and S. M. Parsadaniantz: Highly regionalized distribution of stromal cell-derived factor-1/CXCL12 in adult rat brain: constitutive expression in cholinergic, dopaminergic and vasopressinergic neurons. *European Journal of Neuroscience*, 18(6), 1593-1606 (2003)

34. T. N. Tham, F. Lazarini, I. A. Franceschini, F. Lachapelle, A. Amara and M. Dubois-Dalcq: Developmental pattern of expression of the alpha chemokine stromal cell-derived factor 1 in the rat central nervous system. *Eur J Neurosci*, 13(5), 845-56 (2001)

35. Y. Vagima, K. Lapid, O. Kollet, P. Goichberg, R. Alon and T. Lapidot: Pathways implicated in stem cell migration: the SDF-1/CXCR4 axis. *Natural Killer Cell Protocols*, 750, 277-89 (2011)

36. C. V. Borlongan, M. Hadman, C. D. Sanberg and P. R. Sanberg: Central nervous system entry of peripherally injected umbilical cord blood cells is not required for neuroprotection in stroke. *Stroke*, 35(10), 2385-2389 (2004)

37. M. B. Newman, A. E. Willing, J. J. Manresa, C. D. Sanberg and P. R. Sanberg: Cytokines produced by cultured human umbilical cord blood (HUCB) cells: implications for brain repair. *Exp Neurol*, 199(1), 201-8 (2006)

38. C. J. Barnum and M. G. Tansey: Modeling neuroinflammatory pathogenesis of Parkinson's disease. *Prog Brain Res*, 184, 113-32 (2010)

39. P. L. McGeer and E. G. McGeer: Glial reactions in Parkinson's disease. *Mov Disord*, 23(4), 474-83 (2008)

40. J. D. Adams, Jr., P. W. Kalivas and C. A. Miller: The acute histopathology of MPTP in the mouse CNS. *Brain Res Bull*, 23(1-2), 1-17 (1989)

41. Y. X. Chao, B. P. He and S. S. Tay: Mesenchymal stem cell transplantation attenuates blood brain barrier damage and neuroinflammation and protects dopaminergic neurons against MPTP toxicity in the substantia nigra in a model of Parkinson's disease. *J Neuroimmunol*, 216(1-2), 39-50 (2009)

42. M. Al-Jarrah, M. Jamous, K. Al Zailaey and S. O. Bweir: Endurance exercise training promotes angiogenesis in the brain of chronic/progressive mouse model of Parkinson's Disease. *NeuroRehabilitation*, 26(4), 369-73 (2010)

43. E. Guatteo, S. Marinelli, R. Geracitano, A. Tozzi, M. Federici, G. Bernardi and N. B. Mercuri: Dopamine-containing neurons are silenced by energy deprivation: a defensive response or beginning of cell death? *Neurotoxicology*, 26(5), 857-68 (2005)

44. M. Hadjiconstantinou, A. J. Yates and N. H. Neff: Hypoxia-induced neurotransmitter deficits in neonatal rats are partially corrected by exogenous GM1 ganglioside. *J Neurochem*, 55(3), 864-9 (1990)

45. E. A. Winkler, R. D. Bell and B. V. Zlokovic: Central nervous system pericytes in health and disease. *Nat Neurosci*, 14(11), 1398-405 (2011)

46. M. A. Font, A. Arboix and J. Krupinski: Angiogenesis, neurogenesis and neuroplasticity in ischemic stroke. *Curr Cardiol Rev*, 6(3), 238-44 (2010)

Abbreviation: HUHSCs, human umbilical cord hematopoietic stem cells; PD, Parkinson's disease; CPu, caudate/putamen; SNc, substantia nigra pars compacta; DA, dopamine; MSCs, mesenchymal stem cells; BBB, blood brain barrier; PBS, phosphate buffer; TPO, thombopoietin; MPTP, 1 methyl-4-phenyl-1, 2, 3, 6-tetrahyropyrine; TH, tyrosine hydroxylase; AAAD, aromatic L-amino acid decarboxylase; GFAP, glial fibrillary acid protein; OD, optical density; HPF, high-power field

Key Words: Umbilical Cord. Stem Cells, Parkinson's Disease, Neuron, Regeneration

Send correspondence to: Hiranmoy Das, Dept of Internal Medicine, Director, Cardiovascular Stem Cell Laboratories, The Dorothy M. Davis Heart and Lung Research Institute, The Ohio State University Medical Center, 460 W 12th Avenue, BRT 394, Columbus, Ohio 43210, Tel: 614- 688-8711, Fax: 614-293-5614, E-mail: hiranmoy.das@osumc.edu